

Density profiles for atomic quantum Hall states

N.R. Cooper,¹ F.J.M. van Lankvelt,^{2,*} J.W. Reijnders² and K. Schoutens²

¹*Cavendish Laboratory, Madingley Road, Cambridge CB3 0HE, United Kingdom*

²*Institute for Theoretical Physics, University of Amsterdam, Valckenierstraat 65, 1018 XE Amsterdam, the Netherlands*

(Dated: 1 September, 2004)

We analyze density profiles for atomic quantum Hall states, which are expected to form in systems of rotating cold atoms in the high-rotation limit. For a two-dimensional (single-layer) system we predict a density landscape showing plateaus at quantized densities, signaling the formation of incompressible groundstates. For a set-up with parallel, coupled layers, we predict (i) at intermediate values of the inter-layer tunneling: a continuously varying density profile $\rho(z)$ across the layers, showing cusps at specific positions, (ii) at small values for the tunneling, quantum Hall-Mott phases, with individual layers at sharply quantized particle number, and plateaus in the density profile $\rho(z)$.

PACS numbers: 03.75.Lm, 73.43.Cd

Among the fascinating developments in the field of quantum gases is the possibility to study correlated states of matter in a setting that is entirely different from the traditional setting of electrons in a solid state environment. A prime example are fractional quantum Hall (qH) states, which are expected when trapped atoms (bosons or fermions) are made to rotate at ultra-high angular momentum^{1,2,3,4,5,6,7}. While there has been steady progress in achieving high rotation rates⁸, the conditions for the actual realization of these states have not yet been met. [See^{9,10} for alternative proposals aimed at conditions where atomic qH states are expected.]

The most direct experimental signature of electronic (fractional) qH states, the quantization of the Hall conductance, is not easily available for realizations of such states with neutral atoms. It is thus important to investigate the observable features of atomic qH states. Earlier studies have focused on the fractional statistics¹¹, loss of condensate fraction¹², properties of edge excitations¹³, and on density correlations in expansion images¹⁴.

In this Letter, we work out the proposals put forward in^{15,16} for the detection of atomic (fractional) qH states via characteristic density profiles. We present results for a single layer, and for multi-layer configurations. We shall focus on the fractional qH states formed of interacting bosons, although qualitatively similar results would be obtained for the fractional qH states of interacting fermions. We remark that non-interacting fermions in a rapid rotation regime, and subject to a slowly varying potential, will display density profiles similar to the ones we discuss here¹⁷. In that case, the effects arise from the Landau level structure for non-interacting fermions. All results discussed in the present work are strong many-body interaction effects.

We first analyze a single layer situation, with rotation at or near the critical frequency ω_{\perp} . The char-

acteristic length scales ℓ_{\perp} and ℓ_{\parallel} are set by the harmonic confinement ω_{\perp} in the $x - y$ (in-plane) direction and ω_{\parallel} in the z (out-of-plane) direction, according to $\ell_{\perp, \parallel} = \sqrt{\hbar/(m\omega_{\perp, \parallel})}$. The energy scale characterizing the qH states is $g_{\text{qH}} = \frac{1}{(2\pi)^{3/2}} \frac{4\pi\hbar^2 a_s}{m\ell_{\parallel}\ell_{\perp}^2}$ with a_s the scattering length. Assuming $a_s = 5$ nm, $\hbar\omega_{\perp} \simeq 5$ nK, $\ell_{\parallel} = 50$ nm, g_{qH} is in the order of 1 nK.

The state of matter formed by rapidly rotating bosonic atoms, at critical rotation $\omega = \omega_{\perp}$ and in the absence of any additional potential, depends on the filling fraction $\nu \equiv n/n_0$ [$n_0 \equiv 1/\pi\ell_{\perp}^2$]³. For ν less than $\nu_c \sim 6$, the vortex lattice is unstable^{3,18}, and the groundstates are homogeneous quantum fluids. Their interaction energy density $e[\nu]$ is a complicated function of ν , containing cusps that indicate incompressible groundstates at specific filling fractions ν_i . The incompressible groundstates have been studied by exact diagonalization studies in edge-less geometries (sphere or torus), where it was found that they are well-described by a variety of (fractional) qH liquids^{1,2,3,4,5,7}. These include the Laughlin state at $\nu = 1/2$, a series of states at $\nu^{(p)} = p/(p+1)$ that can be understood in terms of composite fermions (CF)², and non-abelian states such as the Moore-Read (MR) and Read-Rezayi (RR) states¹⁹ at $\nu = k/2$.

Here we focus on inhomogeneous qH liquids that form in the presence of a residual potential $V(r)$ in the rotating frame of reference. We consider (i) rotation ω slightly below the critical frequency ω_{\perp} , leaving a residual parabolic potential $V_2(r) = \frac{1}{2}k_2r^2$ with $k_2 \propto (\omega_{\perp} - \omega)$, (ii) critical rotation $\omega = \omega_{\perp}$, with an additional confining potential, here taken to be quartic, $V_4(r) = \frac{1}{4}k_4r^4$. We shall discuss first the case in which there is a very large number of atoms, $N \gg 1$, in which case mean density profiles can be reliably found from a one-shot measurement of particle positions; we shall then turn to discuss the effects of fluctuations when N is not very large.

If the potential $V(r)$ varies slowly in space compared to ℓ_{\perp} , the density distribution, $n(r)$, averaged on scales

*address from Oct. 2004: Rudolf Peierls Centre for Theoretical Physics, 1 Keble Road, Oxford OX1 3NP, England

large compared to ℓ_{\perp} , can be obtained by minimizing

$$E = \int d^2r \{e[\nu(r)] + V(r)n(r) - \mu n(r)\}, \quad (1)$$

where $e[\nu]$ is the interaction energy density arising from the contact interactions, $\nu(r) \equiv n(r)/n_0$ and μ is the chemical potential. That the energy functional (1) is local significantly simplifies its minimization: at each position, the density $n(r)$ is that which minimizes $e[\nu(r)] - \mu_L n(r)$, where the local chemical potential is $\mu_L(r) \equiv \mu - V(r)$. For a vortex lattice (at large ν), the energy density is $e[\nu] = n_0 \nu^2 b g_{\text{qH}}$, where $b = 1.1596$ is the Abrikosov parameter for a triangular lattice. The dependence of density on $\mu_L(r)$ is then simply $n(r) \propto \mu_L(r)$, leading to a Thomas-Fermi profile.²⁰ For the qH regime, $\nu < \nu_c$, there are cusps in the energy function $e[\nu]$, which give rise to a step-like dependence of n on μ_L ; this causes plateaus in the spatial density distribution.

As a simple example, we consider a situation where liquids at $\nu = 1/2$ and $\nu = 2/3$ make up the lowest energy configuration. The energy per unit area takes the values $e[\nu = 1/2] = 0$, and $e[\nu = 2/3] = (2/3)n_0\epsilon_2$ (with ϵ_2 a number of order g_{qH} , see⁴). We find $\nu = 0$ for $\mu < 0$, $\nu = 1/2$ for $0 < \mu < 4\epsilon_2$, and $\nu = 2/3$ for $\mu > 4\epsilon_2$.

Let us take a harmonic confining potential $V(r) = \frac{1}{2}k_2 r^2$, such that $\mu_L(r) = \mu - \frac{1}{2}k_2 r^2$. The $\nu = 1/2$ state forms a disc that extends out to $\mu_L = 0$, *i.e.* to a radius $r_1 = \sqrt{2\mu/k_2}$. There is a critical value of chemical potential, $\mu_c = 4\epsilon_2$, at which the $\nu = 2/3$ state will first appear in the center of the trap (where μ_L is maximum). At $\mu = \mu_c$, the number of atoms in the $\nu = 1/2$ disc is $N_c = 1/2 n_0 \pi r_1^2 = 2\epsilon_2/\lambda_2$, with $\lambda_2 = \frac{1}{2}k_2 \ell_{\perp}^2$. Above this critical value, the inner disc at $\nu = 2/3$ has a radius $r_2 = \sqrt{2(\mu - \mu_c)/k_2}$. Expressed in terms of N and N_c , the locations of the two steps are $r_2/\ell_{\perp} = \sqrt{3(N - N_c)}/2$, $r_1/\ell_{\perp} = \sqrt{(3N + N_c)}/2$. From the dependence $e[\nu]$ obtained from exact diagonalizations³ it can be inferred that intermediate densities other than $\nu = 0, 1/2, 2/3$ will not appear in the density profile.

Repeating this analysis in a quartic potential $V_4(r) = \frac{1}{4}k_4 r^4$ leads to a critical N of $N_c = \sqrt{\epsilon_2/\lambda_4}$, with $\lambda_4 = \frac{1}{4}k_4 \ell_{\perp}^4$, with inner and outer edges at $(r_2/\ell_{\perp})^2 = \frac{3}{4}(\sqrt{9N^2 - 8N_c^2} - N)$, $(r_1/\ell_{\perp})^2 = \frac{9}{4}N - \frac{1}{4}\sqrt{9N^2 - 8N_c^2}$.

Including in the analysis more quantum liquids, at filling $\nu_1 < \nu_2 < \dots$, leads to a sequence of critical values $N = N_c^{(k)}$, marking the onset of the formation of a central region of a qH fluid at $\nu = \nu_k$. To determine the corresponding density profiles we use the interaction energy function $e[\nu]$ calculated by exact diagonalization studies on a torus³. In the graphs presented in Fig. 1, a confining potential $V(r) = \frac{1}{2}k_2 r^2$ is assumed. The energy functions used are for a system size of $N_V = 6$ single-particle states on a torus with aspect ratio $\sqrt{3}/2$ (solid lines) [with numerical results up to $\nu = \frac{25}{3}$], and for $N_V = 12$ single-particle states on a torus with aspect ratio 0.3 (dashed lines) [up to $\nu = \frac{7}{6}$]. For filling fractions larger than $\nu_c \sim 6$, the groundstate is a compressible vor-

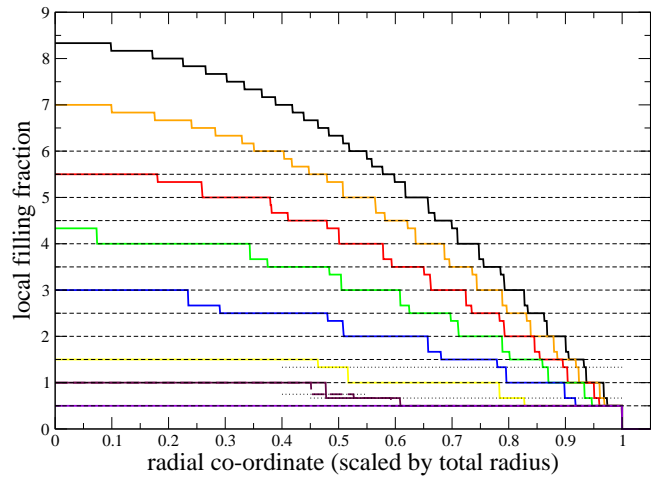


FIG. 1: Radial density profiles in a single layer with harmonic confinement, for a series of filling fractions at the center of the trap. The solid and dashed lines correspond to energy functions $e[\nu]$ obtained from numerics using $N_V = 6$ and $N_V = 12$ states, respectively.

tex lattice³. In this regime, the density profile (averaged on a lengthscale large compared to ℓ_{\perp}) is an inverted parabola²⁰. The steps seen in Fig. 1 in this regime are an artifact of the finite-size numerics (on a finite system with $N_V = 6$ the minimum change of filling fraction is $\Delta\nu = 1/6$). For filling fractions less than $\nu_c \sim 6$, plateaus appear at the filling fractions of incompressible qH fluids, including the sequence of MR and RR states at $\nu = k/2$ [horizontal dashed lines] as well as some of the CF sequence $\nu = p/(p+1)$ with $p = 2, 3, -4$ [dotted lines]. This plateau structure is a direct consequence of the incompressibility of the fractional quantum Hall liquids. This structure could be observed in the density distribution of a single-layer system following expansion¹⁴.

We have tested the above picture against exact diagonalization results for small systems. However, at the small sizes that can be handled in exact diagonalization (up to $N = 12$ particles on a disc), the density profiles seem to be dominated by edge effects, indicating that the system sizes do not exceed the correlation lengths in the expected qH liquids²¹.

We next investigate the situation where an optical lattice in the z direction is imposed on a cloud of atoms rotating around the z -axis.²² If the optical potential is sufficiently deep, this will define a stack of parallel planes with (weak) tunneling t between the planes. The lengthscale ℓ_{\parallel} is now determined by the confinement frequency in a single layer of the optical lattice. We assume that there is an overall quadratic confinement in the z -direction, giving rise to a chemical potential $\mu(z) = \mu_0 - \mu_2(z/d)^2$ (with d the distance between the layers), which will induce a slow modulation in the number of particles per layer. The idea is that parameters can be chosen such that, while the original cloud is in a mean field regime ($\nu > \nu_c$), displaying a vortex lattice, the individual lay-

ers defined by the optical lattice can be in a quantum regime, so that the entire configuration becomes a stack of weakly coupled quantum liquids. With N_L layers, a total filling fraction ν (for the entire cloud) gives a filling fraction per layer of $\nu' = \nu/N_L$. If $\nu' < \nu_c$, the vortex lattice will melt if the inter-layer tunneling energy t is made smaller than a critical value t_{c1} . We have generalized the analysis of¹⁸ to determine the value of t_{c1} (see²¹ for a detailed account). For $N = 5000$ particles, $N_V = 100$ vortices and a number of layers $N_L = 50$, our estimate is $t_{c1} \sim 0.1 g_{\text{qH}}$.

Assuming $N/N_L \gg 1$ and $t \ll g_{\text{qH}}$ we have the following physical picture. Within each layer, we have a density landscape built out of incompressible qH liquids each of the form shown in Fig. 1. This landscape varies slowly from layer to layer. The gap for bulk excitations over each qH liquid is of order g_{qH} ^{3,4} and since $t \ll g_{\text{qH}}$ there will be no ‘bulk-to-bulk’ tunneling events between the layers. However, the energy scale for processes where atoms tunnel from the edge of a qH fluid in one layer i to the corresponding edge in an adjacent layer $i \pm 1$, is much lower, of order g_{Mott} . This scale is defined as $g_{\text{Mott}} \simeq \lambda_2$ for quadratic confinement and $g_{\text{Mott}} \simeq \lambda_4 N_i$ for the quartic case, with N_i the number of particles in the qH liquid in layer i . In terms of $N_0 = g_{\text{qH}}/\lambda_2$ ($N_0 = \sqrt{g_{\text{qH}}/\lambda_4}$) we have $g_{\text{Mott}} \simeq g_{\text{qH}}/N_0$ ($g_{\text{Mott}} \simeq g_{\text{qH}} N_i/N_0^2$) for the quadratic (quartic) case. If the tunneling t is large on the scale of g_{Mott} , inter-layer tunneling events will establish a continuously varying density profile $\rho(z) = \langle N_i \rangle$ across the layers (where N_i is now the total number of particles in layer i). This profile could be measured from an image of the confined condensate, provided the period of the lattice, d , is made larger than the imaging resolution (perhaps by forming the optical potential from running waves at a shallow angle).²³

We first assume quadratic in-plane confinement. If the number of particles per layer stays below $N_c^{(2)} = 2\epsilon_2/\lambda_2$, the qH liquids in the layers will be Laughlin liquids at $\nu = 1/2$. Minimizing the total energy w.r.t. each of the N_i , we obtain a parabolic TF density profile

$$\rho(z) = \frac{1}{d^2} \frac{\mu_2}{2\lambda_2} (z_1^2 - z^2), \quad (2)$$

with $z_1^3 = d^3 \frac{3N}{2} \frac{\lambda_2}{\mu_2}$. If N, μ_2 are such that some of the N_i exceed the critical values $N_c^{(k)}$, there will be additional stable qH liquids in these layers. The corresponding profile $\rho(z)$ exhibits cusps at the positions $\pm z_k$ where N_i goes through $N_c^{(k)}$. If the central layers near $z = 0$ support $\nu = 1/2$ and $\nu = 2/3$ liquids, we have

$$\begin{aligned} \rho(z) &= \frac{1}{d^2} \frac{\mu_2}{2\lambda_2} (z_1^2 - z^2) \quad \text{for } z_2 < |z| < z_1 \\ &= N_c^{(2)} + \frac{1}{2d^2} \frac{2\mu_2}{3\lambda_2} (z_2^2 - z^2) \quad \text{for } |z| < z_2 \end{aligned} \quad (3)$$

with $z_1^2 - z_2^2 = 2d^2 N_c \frac{\lambda_2}{\mu_2}$ and $z_1^3 + z_2^3/3 = d^3 \frac{3N}{2} \frac{\lambda_2}{\mu_2}$. This profile shows a (weak) cusp at $|z| = z_2$, with the slope $\frac{\partial}{\partial z} \rho(z)$ changing by a factor of 4/3.

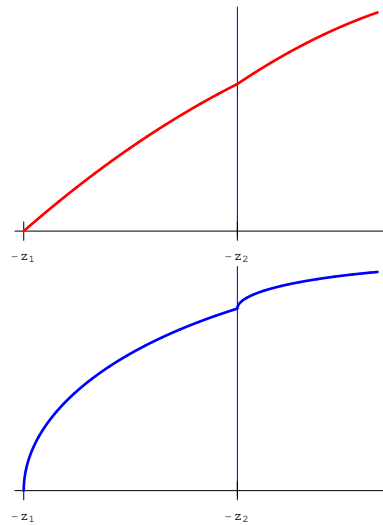


FIG. 2: Density profiles $\rho(z)$ for quadratic (top) and quartic (bottom) in-plane confinement. The layers at $-z_1 < z < -z_2$ have the $\nu_1 = 1/2$ liquid only; the cusps at $z = -z_2$ mark the onset of a second liquid with $\nu_2 = 2/3$ in the layers.

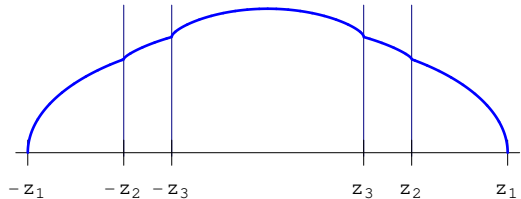


FIG. 3: Schematic density profile $\rho(z)$, for quartic in-plane confinement and qH liquids at $\nu_1 = 1/2$, $\nu_2 = 2/3$, $\nu_3 = 1$.

The nature of the cusps at $z = z_k$ depends on the in-plane potential $V(r)$. In Fig. 2 we show the cusp at $z = -z_2$ for two choices of $V(r)$. Clearly, a steeper confinement in the layers leads to a more pronounced cusp in the profile $\rho(z)$. [A square well cut-off in $V(r)$ can produce a flat plateau in $\rho(r)$.] For quartic confinement, the profile at $N < N_c^{(2)}$ is a semi-circle, and the cusps at $|z| = z_k$ have square-root singularities. In fact, $\rho(z)$ is of the general form $\rho(z) = \sum_k a_k \sqrt{z_k^2 - z^2}$. Fig. 3 shows $\rho(z)$ for quartic confinement, with the layers supporting quantum liquids at $\nu_1 = 1/2$, $\nu_2 = 2/3$, $\nu_3 = 1$. (We note in passing that similar considerations lead to the conclusion that the density distribution following an *expansion* of a multi-layered system in an otherwise quadratically-confined trap will have a dependence on the radial co-ordinate r that is of the same qualitative form as Fig. 3 is of the axial co-ordinate z .)

We now turn to consider the situation when N is not very much larger than 1. We begin by estimating the fluctuations. A deviation δN_i from the mean field profile costs an energy of order $g_{\text{Mott}} (\delta N_i)^2$, giving

$$\delta N_i \simeq \sqrt{N_0 \frac{t}{g_{\text{qH}}}}, \quad \delta N_i \simeq \sqrt{\frac{N_0^2}{N_i} \frac{t}{g_{\text{qH}}}} \quad (4)$$

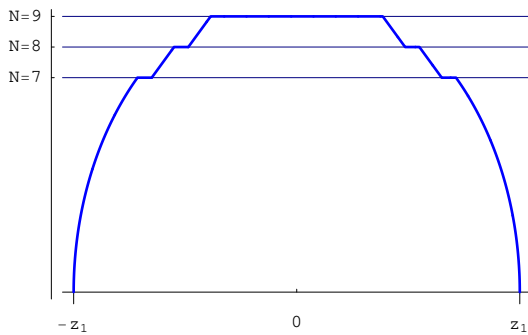


FIG. 4: Schematic density-profile $\rho(z)$, for layers supporting Laughlin liquids in quartic confinement. The horizontal segments indicate the qH-Mott phases, with sharply quantized particle number per layer, while the remaining parts correspond to ‘conducting’ phases, with fluctuating N_i .

for the quadratic and quartic cases. In addition there will be intra-layer fluctuations, for example when a particle at radius r_i is promoted to an unoccupied orbital at $r_i + \delta r_i$. Equating the corresponding energy to t leads to

$$\frac{\langle \delta r_i \rangle}{r_i} \simeq \frac{N_0}{N_i} \frac{t}{g_{\text{qH}}}, \quad \frac{\langle \delta r_i \rangle}{r_i} \simeq \left(\frac{N_0}{N_i} \right)^2 \frac{t}{g_{\text{qH}}} \quad (5)$$

for the quadratic and quartic cases. This shows that if $t \ll g_{\text{qH}}$ and N_i/N_0 is not too small, the steps in the in-layer density profiles are well-defined on the scale of the overall radius.

A one shot experiment will obviously produce integer values for all N_i . Based on the above, we predict that these numbers will follow our continuous curves for $\rho(z)$

rather closely, with fluctuations as specified in Eq. (4). Gradually lowering t (for example, by turning on the potential slowly enough) will lead to values N_i that are nearest integers to the corresponding values of $\rho(z)$.

The estimates in Eq. (4) indicate that $\delta N_i \simeq 1$ if t is lowered to a value of order g_{Mott} . Based on the analogy with single atoms in an optical lattice, we anticipate a Mott phase where the numbers N_i are sharply quantized. We have analyzed an effective Bose-Hubbard model, with layers supporting a $\nu = 1/2$ state in quadratic confinement. In a mean-field treatment we find, for μ satisfying $2\lambda_2(N-1) < \mu < 2\lambda_2 N$, the following critical t for entering the N -particle qH-Mott phase

$$t_{c_2}(N) = -\lambda_2 \left[N - \frac{\mu}{2\lambda_2} \right] \left[(N-1) - \frac{\mu}{2\lambda_2} \right]. \quad (6)$$

This has a maximum of $\lambda_2/4$, which is of order g_{Mott} , for all N . For confinement ‘steeper than’ quadratic, the maximal $t_{c_2}(N)$ grows with N , consistent with $g_{\text{Mott}} \simeq \lambda_4 N$ for the quartic case.

Scanning the sample from layer to layer, there will then be segments showing qH-Mott phases, and ‘conducting’ regions in between, see Fig. 4. A measurement of the particle number per layer in an N -particle qH-Mott phase will give $N_i = N$ with no fluctuations. The same measurement in a ‘conducting’ phase will produce integer numbers as well, but these will show fluctuations.

We thank J. Dalibard and V. Schweikhard for illuminating discussions. FJMvL thanks Brookhaven Nat. Lab. for hospitality. This research was supported by EPSRC grant GR/S61263/01 (NRC) and by NWO and FOM of the Netherlands (FJMvL, JWR, KS).

-
- ¹ N.K. Wilkin, J.M.F. Gunn, R.A. Smith, Phys. Rev. Lett. **80**, 2265 (1998); N.K. Wilkin, J.M.F. Gunn, Phys. Rev. Lett. **84**, 6 (2000).
² N.R. Cooper, N.K. Wilkin, Phys. Rev. **60**, R16279 (1999).
³ N.R. Cooper, N.K. Wilkin, J.M.F. Gunn, Phys. Rev. Lett. **87**, 120405 (2001).
⁴ N. Regnault, Th. Jolicoeur, Phys. Rev. Lett. **91**, 030402 (2003); cond-mat/0404093; cond-mat/0406013.
⁵ T.-L. Ho, E.J. Mueller, Phys. Rev. Lett. **89**, 050401 (2002).
⁶ B. Paredes, P. Zoller, J.I. Cirac, Phys. Rev. A **66**, 033609 (2002).
⁷ J.W. Reijnders *et al.*, Phys. Rev. Lett. **89**, 120401 (2002); Phys. Rev. A **69**, 023612 (2003).
⁸ V. Bretin *et al.*, Phys. Rev. Lett. **92**, 050403 (2004); V. Schweikhard *et al.*, Phys. Rev. Lett. **92**, 040404 (2004).
⁹ E.J. Mueller, cond-mat/0404306; A. Sørensen, E. Demler, M. Lukin, cond-mat/0405079;
¹⁰ M. Popp, B. Paredes, J.I. Cirac, cond-mat/0405195.
¹¹ B. Paredes *et al.*, Phys. Rev. Lett. **87**, 010402 (2001).
¹² J. Sinova, C.B. Hanna, A.H. MacDonald, Phys. Rev. Lett. **90**, 120401 (2003).
¹³ M.A. Cazalilla, Phys. Rev. A **67**, 063613 (2003); M.A. Cazalilla, N. Barberán, cond-mat/0408540.
¹⁴ N. Read, N.R. Cooper, Phys. Rev. A **68**, 035601 (2003); E. Altman, E. Demler, M.D. Lukin, cond-mat/03096226.
¹⁵ F.J.M. van Lankvelt, J.W. Reijnders, K. Schoutens, presentation S3.003 at 2004 APS March Meeting (Montreal).
¹⁶ N.R. Cooper, presentation at the conference ‘Quantum Gases’ KITP Santa Barbara (May 2004).
¹⁷ T.-L. Ho, C.V. Ciobanu, Phys. Rev. Lett. **85**, 4648 (2000).
¹⁸ J. Sinova, C.B. Hanna, A.H. MacDonald, Phys. Rev. Lett. **89**, 030403 (2002).
¹⁹ G. Moore, N. Read, Nucl. Phys. **B 360**, 362 (1991); N. Read, E. Rezayi, Phys. Rev. B **59**, 8084 (1999).
²⁰ G. Watanabe, G. Baym, C.J. Pethick cond-mat/0403470; N.R. Cooper, S. Komineas, N. Read cond-mat/0404112.
²¹ N.R. Cooper, F.J.M. van Lankvelt, J.W. Reijnders and K. Schoutens, manuscript in preparation.
²² The authors were first made aware of this proposal by E. Cornell.
²³ The authors learned of this proposal from J. Dalibard.